

# Tool life and surface integrity when turning titanium aluminides with PCD tools under conventional wet cutting and cryogenic cooling

Paolo C. Priarone<sup>1</sup> · Fritz Klocke<sup>2</sup> · Maria Giulia Faga<sup>3</sup> · Dieter Lung<sup>2</sup> · Luca Settineri<sup>1</sup>

Received: 3 July 2015 / Accepted: 8 October 2015  
© Springer-Verlag London 2015

**Abstract** The high-performance machining of difficult-to-cut alloys requires the development and optimization of high-performance tools, able to withstand the thermo-mechanical tool load without compromising the surface quality of produced components. In this context, the machinability of titanium aluminides still represents a demanding challenge. In this paper, the performance of cubic boron nitride (CBN) and polycrystalline diamond (PCD) cutting inserts is compared to that of uncoated and coated carbide tools. Longitudinal external turning tests were performed on a Ti-43.5Al-4Nb-1Mo-0.1B (TNM) at.% cast and hot isostatically pressed (HIPed)  $\gamma$ -TiAl alloy, by using a conventional lubrication supply. In addition, PCD tools were also applied under cryogenic cooling with liquid nitrogen. Results proved that PCD cutting tools have the potential to improve the machining productivity of titanium aluminides, due to their high hardness and excellent thermal conductivity. A noteworthy further increase of tool life was possible by using PCD cutting inserts under cryogenic cooling conditions.

**Keywords** PCD · CBN · High-performance cutting · Titanium aluminide · Cryogenic-assisted cutting · Surface integrity

## 1 Introduction

Advanced lightweight and thermally stable alloys have been receiving an increasing industrial attention. In this scenario, titanium aluminides (TiAl) were identified as alternative to more traditional materials for thermally and mechanically stressed components [1]. These materials are basically compounds formed from two metals, titanium and aluminum, showing structures and properties completely different from their basic constituents. In addition, alloying elements improve properties as ductility, strength, and creep and oxidation resistance [2]. Titanium aluminides exist in different phases, but only the  $\alpha_2$  (Ti<sub>3</sub>Al) and  $\gamma$  (TiAl) phases are of interest. Such phases by themselves have scarce engineering significance, but a combination of them, which exists between 40 and 48 at.% of Al content, has proved to be valuable for structural applications. TiAl intermetallic alloys have an attractive combination of strength-to-weight ratio (being the density of titanium aluminides approximately half that of nickel-based superalloys), refractoriness, oxidation resistance, high elastic modulus, strength retention at high temperatures, and good creep resistance [3, 4]. Commercial interest is centered mainly in aerospace and automotive sectors, and possible fields of application can be detected in both rotating and non-rotating parts. Low-pressure turbine blades, compressor vanes, swirl nozzles, automotive engine valves, and turbochargers could be made of these alloys [5–8]. Investment casting, ingot metallurgy, and powder metallurgy [9, 10], usually coupled with a series of post-processing steps (as hot isostatic pressing, aging, annealing, and hot working) were used to produce TiAl parts. Several thermo-mechanical routes as hot rolling, forging, and extrusion were also utilized [11, 12]. Moreover, aiming to reduce the post-processing steps, some advanced techniques as direct rolling, laser forming, spark plasma sintering, and mechanical alloying were applied, as highlighted by Kothari et al. [3].

---

✉ Paolo C. Priarone  
paoloclaudio.priarone@polito.it

<sup>1</sup> Department of Management and Production Engineering, Politecnico di Torino, Corso Duca degli Abruzzi 24, 10129 Torino, Italy

<sup>2</sup> Laboratory for Machine Tools and Production Engineering (WZL), RWTH Aachen University, Manfred-Weck Haus, Steinbachstraße 19, 52026 Aachen, Germany

<sup>3</sup> Imamoter, National Research Council (CNR), Strada delle Cacce 73, 10135 Torino, Italy

As far as machining is concerned, titanium aluminides are classified as difficult-to-cut materials (more than standard titanium alloys), because of their high hardness and brittleness, low thermal conductivity, strong tendency to hardening, and high chemical reactivity [13, 14]. On the workpiece side, these characteristics result into residual stresses and surface damage with poor finish [15, 16]. One of the key problems related to the poor machinability of these materials is the formation of defects in the form of microcracks and microfractures on the workpiece surfaces [17, 18]. Such defects may act as the initial point for crack propagation resulting in part failure, which is completely unacceptable for safety critical components, whereas surface integrity is indispensable. Nevertheless, the influence of surface and subsurface defects on fatigue life might be reduced by the compressive residual stress near the surface due to the cutting process and/or by the deformation of the lamellae restricting crack growth [19, 20]. Literature still lacks information about machining performance whether involving conventional or non-conventional processes. This is apparently in contrast to the numerous publications regarding development/processing of TiAl alloys, fatigue behavior, microstructure and mechanical properties, oxidation, and thermal protection. Moreover, the extremely challenging machining of titanium aluminides is one of the major reasons that so far these alloys are hardly used in series products.

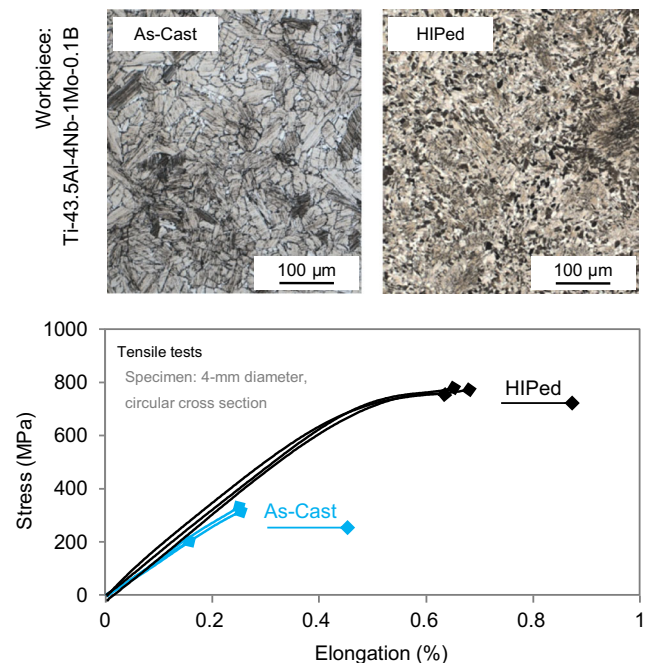
Focusing on cutting operations with defined cutting edges, a limited number of publications analyzing processes as turning (e.g., [19–22]), milling (e.g., [23–27]), and drilling (e.g., [28–30]) can be found. In addition, the obtained results are strongly dependent on the specific alloy and its production technology [31]. Hard metals are widely applied [22, 23, 32], even if some attempts using other cutting tool materials were carried out (as reviewed by Aspinwall et al. [13]). Apart from some promising results, workpiece surface integrity requirements are quite far to be achieved, and the machinability with high-performance cutting materials is still an open research task. In this context, diamond is the hardest and most conductive known material. Even if it is usually unsuitable for machining ferrous materials, because of the high chemical affinity between carbon and iron, diamond has a wide range of applications due to its peculiar properties [33, 34]. For instance, ceramics (e.g., zirconia [35]), metal matrix composites, carbon-fiber-reinforced plastics [36], and wood-based composites [37] were successfully machined with diamond-based tools. Polycrystalline diamond (PCD) exists in different grades, depending on the diamond particle size. Abrasion resistance increases when increasing grain size, while edge quality increases when decreasing grain size (under comparable conditions) [38]. Cubic boron nitride (CBN) is another superabrasive cutting material with high hardness, and its potential applications in machining have been widely investigated for several workpiece materials, as Inconel [39] or steels [40]. The machinability of difficult-to-cut materials and, in

particular, of gamma titanium aluminides by using PCD and CBN tools still represents an area to be explored. The research activities presented in the present paper aim to analyze the performance of PCD and CBN tools in comparison to that of uncoated and coated carbide cutting inserts. Tools with different CBN content and PCD inserts with grain size of 2 and 7–10  $\mu\text{m}$  were tested under conventional flood cooling lubrication. Moreover, PCD tools were also applied under cryogenic cooling, as detailed in Sect. 2. Results are discussed in Sect. 3 focusing on tool wear/life and machined surface quality.

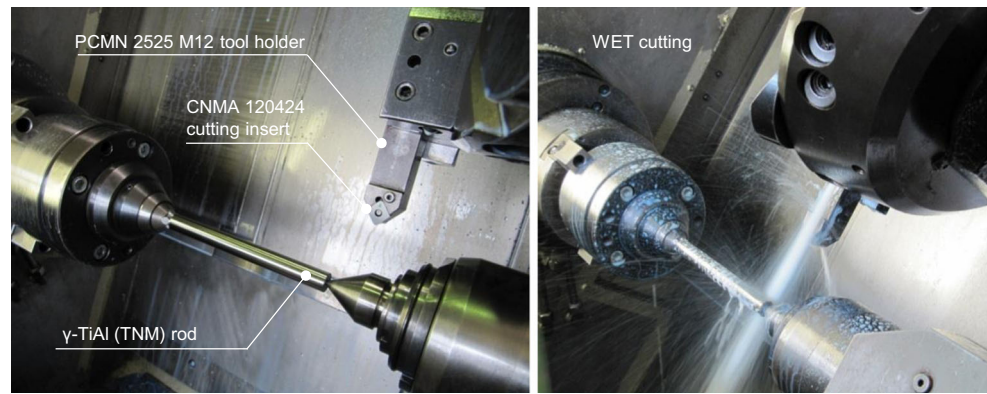
## 2 Experimental approach

### 2.1 Cutting tests

In order to define the influence of different cutting materials on machining performance, experimental trials were carried out. The workpieces were rods of 16-mm diameter and 160-mm length, made of a Ti-43.5Al-4Nb-1Mo-0.1B (TNM) at%  $\gamma$ -TiAl alloy. The rods were produced by Access GmbH (Germany) via an investment casting process [41] and hot isostatically pressed (HIPed) afterward for 6 h at 1185 °C, at a pressure of 172 MPa, in a pure argon atmosphere. The effects of such treatment on the alloy's microstructure and mechanical behavior are highlighted in Fig. 1. Other information concerning the material properties is detailed in [31]. A preliminary rough-turning operation was executed in order to remove the cast skin and to guarantee the cylindricity of the samples.



**Fig. 1** Effects of HIP treatment on microstructure and properties of the TNM alloy [31]

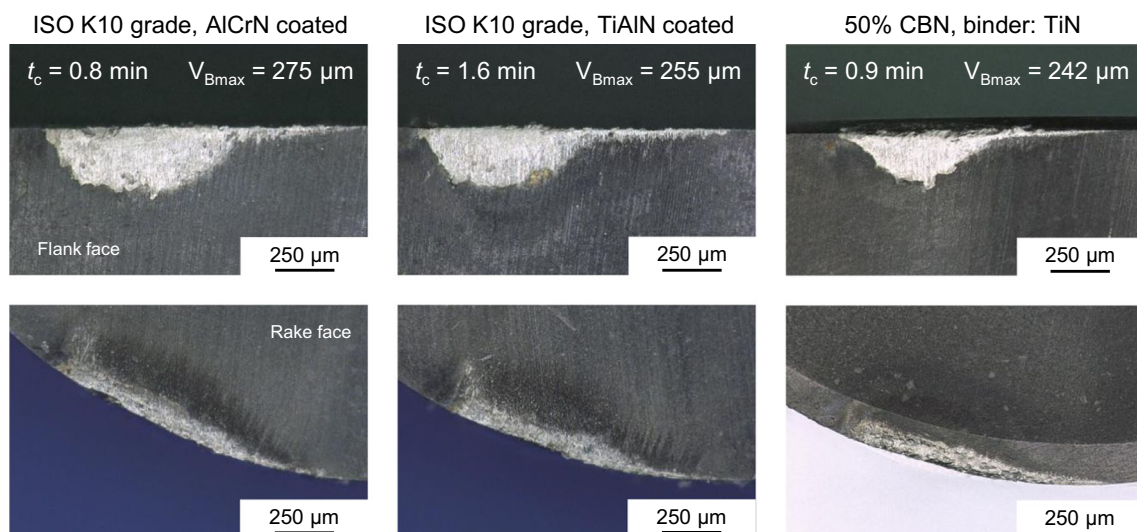
**Fig. 2** Experimental setup for wet cutting

Longitudinal external turning tests were performed on a CNC Index GU 800 lathe. Tool geometry and finishing process parameters were chosen according to previous researches [31, 32]. Cutting speed was  $v_c = 80$  m/min, feed was  $f = 0.1$  mm, and depth of cut was  $a_p = 0.25$  mm. A 6 % emulsion of Fuchs Ecocool TN 2525-HP oil in water, supplied at a pressure of 6 bar, was selected as lubrication condition (conventional flood cooling). Figure 2 shows the experimental setup. The performance of CNMA 120424 coated and uncoated carbide tools, supplied by Febametal S.p.A. (Italy), as well as of cubic boron nitride (CBN) and polycrystalline diamond (PCD) cutting inserts, provided by Cate S.r.l (Italy), was investigated. Cutting inserts with large tool corner radius (equal to 2.4 mm for CNMA 120424 geometry) show lower wear progression and lower surface roughness indices in comparison to those of cutting inserts with small corner radius [32]. Carbide and PCD inserts were sharp, while CBN tools were prepared with a chamfer on the cutting edge ( $\gamma_n = 20^\circ$ ;  $b_{\gamma n} = 125$   $\mu\text{m}$ ). More in detail, carbide ISO K10-grade inserts were tested either uncoated or coated with AlCrN and TiAlN

coatings. Tools with low (50 %) and high (92 %) CBN content were compared, with titanium nitride or titanium carbide binders. PCD was characterized by a grain size of 2 and 7–10  $\mu\text{m}$ . For PCD tools, the grade of bonding determines the tool resistance against abrasive wear, while the size of the crystals determines the sharpness of the cutting edge. The tools produced with small crystals (applied in the present tests) are expected to generate better surface finish than tools produced of large crystals [33]. Tool wear was checked at regular time steps with a Keyence digital microscope, and surface roughness was acquired by a portable tester. The arithmetic mean roughness  $R_a$  and the maximum height of profile  $R_z$  were measured in the feed direction at regular time steps. Worn tools and machined surfaces were observed by means of a scanning electron microscope (SEM).

## 2.2 Characterization of PCD cutting material

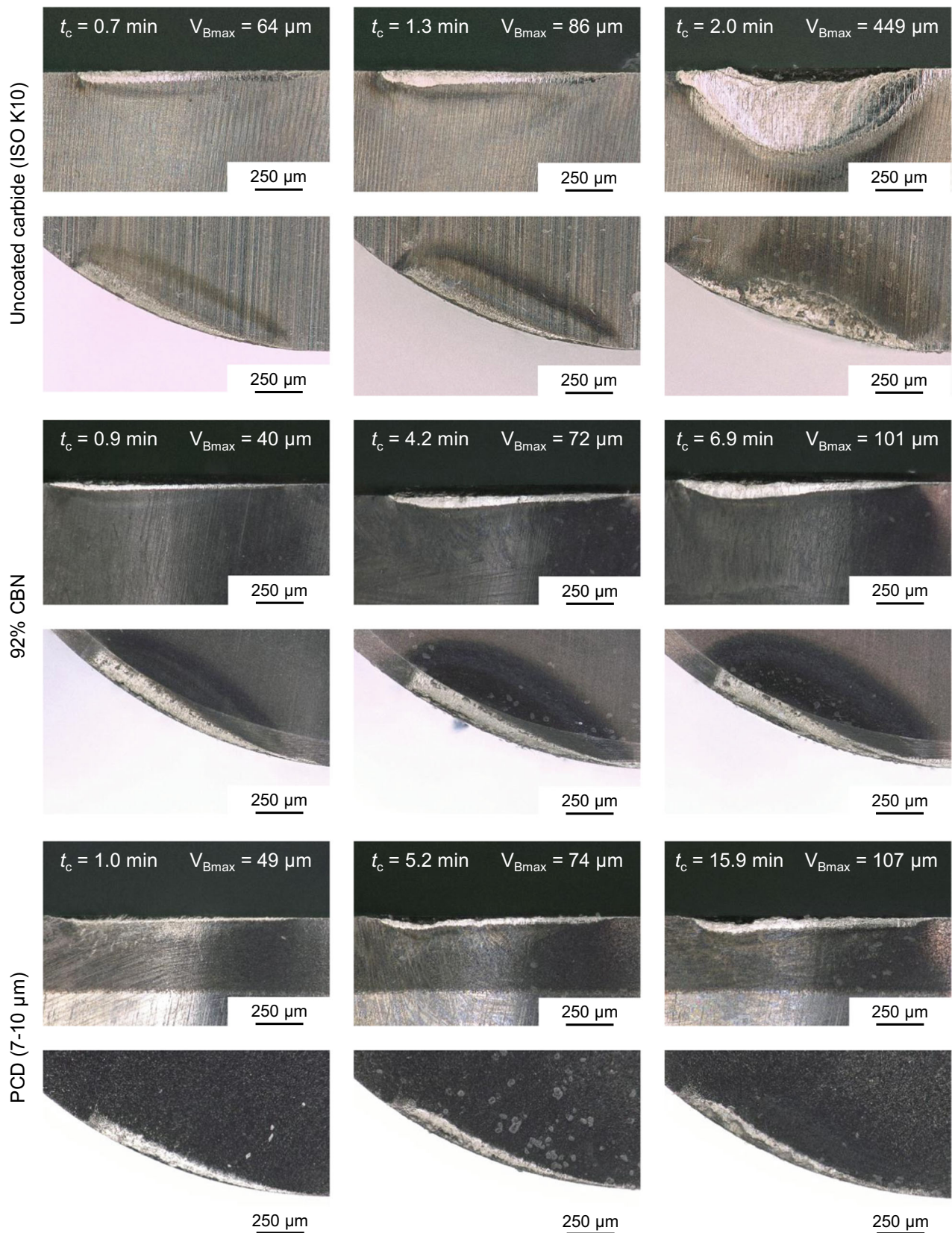
At the end of turning tests, focusing onto the tools which had provided the best performance, a characterization of PCD



Cutting conditions:  $v_c = 80$  m/min;  $f = 0.1$  mm;  $a_p = 0.25$  mm; WET cutting (emulsion)

**Fig. 3** Tool wear observations for coated carbide and low-content CBN cutting inserts



Cutting conditions:  $v_c = 80$  m/min;  $f = 0.1$  mm;  $a_p = 0.25$  mm; WET cutting (emulsion)**Fig. 4** Tool wear observations for uncoated carbide, 92 % CBN, and PCD 7–10- $\mu\text{m}$  cutting inserts

cutting materials was performed. Microhardness and Young modulus were measured by a Fisherscope HM2000XYm nanoindentation tester equipped with the WIN-HCU software. For this tester, the load ranges between 0.4 and 2000 mN, with a resolution of  $4 \cdot 10^{-2}$  mN. A typical Vickers indenter (pyramid shape, with a square base, having a vertex angle of  $136^\circ$ ) was adopted. By using this computer-controlled measuring system, test force and indentation depth were measured and recorded continuously, during increasing and decreasing load. Five measurements were acquired per each sample. In addition, the microstructures were studied by using a Scanning Electron Microscope Zeiss EVO 50 fitted out with an energy dispersion spectroscopy (EDS) analyzer for elemental composition detection. A LaB<sub>6</sub> filament was employed, using secondary and backscattered electrons to acquire the micrographs.

### 2.3 The use of PCD tools under cryogenic cooling

It has already been shown that cryogenic cooling with liquid nitrogen (LN<sub>2</sub>) could be a suitable strategy to enhance cutting performance when turning titanium aluminides [32, 42]. The increase of cooling action due to the extremely low temperature of LN<sub>2</sub> is expected to increase the thermal gradient between cutting zone and tool, thus reducing the thermal load on the cutting edge [32]. This effect, matched with the superior thermal conductivity of diamond [34], should enhance the tool life further. Therefore, longitudinal external turning tests combining PCD tools (with the grain size of 7–10  $\mu\text{m}$ ) and cryogenic cooling were also executed. The Index GU 800 CNC lathe was set up with a LN<sub>2</sub> supply system (as described in [42]), and CNMA 120424 PCD inserts were clamped in an Iscar PCLNL 2525M-12-JHP tool holder designed to direct the LN<sub>2</sub> flow on the rake face of the tool. LN<sub>2</sub> supply pressure was 2 bar, with a flow rate of 2.3 kg/min. The process parameters were unchanged ( $v_c=80$  m/min,  $f=0.1$  mm,  $a_p=0.25$  mm).

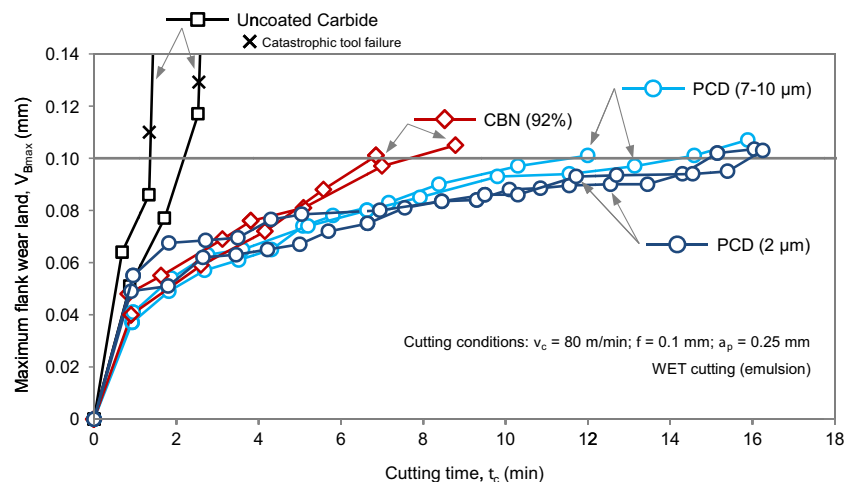
## 3 Results and discussion

### 3.1 Tool wear results under conventional flood cooling

Tests continued until reaching a maximum flank wear land ( $V_{Bmax}$ ) limit of 0.1 mm. The choice of such restrictive value for the wear limit is consistent with previous research studies [31], and it was adopted with the aim of retaining a low tool wear to preserve the surface integrity of the machined parts. The TNM  $\gamma$ -TiAl rods were replaced as the diameter was reduced to 10 mm, in order to avoid dynamic instability problems during the turning process. Experimental evidence demonstrated that a huge tool wear was detected since the beginning of the cutting tests for both AlCrN- and TiAlN-coated carbide tools. Similar results were obtained with 50 % CBN content cutting inserts, in spite of the type of binder (titanium nitride or titanium carbide) used. For all those cutting materials, tool life was less than approximately 1 min (Fig. 3).

For the other cutting materials, tool wear optical images are shown in Fig. 4, and typical tool wear curves are plotted in Fig. 5. It is worth to remark that tool life results are strongly dependent on the workpiece material, as evidenced by the benchmark trials detailed in [31]. The progression of predominantly abrasive wear on the flank side of uncoated carbide inserts is quite regular, up to the achievement of a sudden catastrophic tool failure. A tool life  $T_L$  of approximately 2 min was obtained. CBN and PCD tools have the potential to improve the machinability of titanium aluminides, consequently increasing machining productivity. In particular, thermal conductivity and resistance against abrasive wear increase with increasing CBN content and grain size [43]: 92 % CBN content inserts lead to a more stable process, with average tool life of  $T_L=7.2$  min. Diamond is superior to all the other known materials with respect to hardness and thermal conductivity [34]. An increase in tool life up to  $T_L \approx 14$  min was obtained

**Fig. 5** Influence of cutting material on tool wear curves



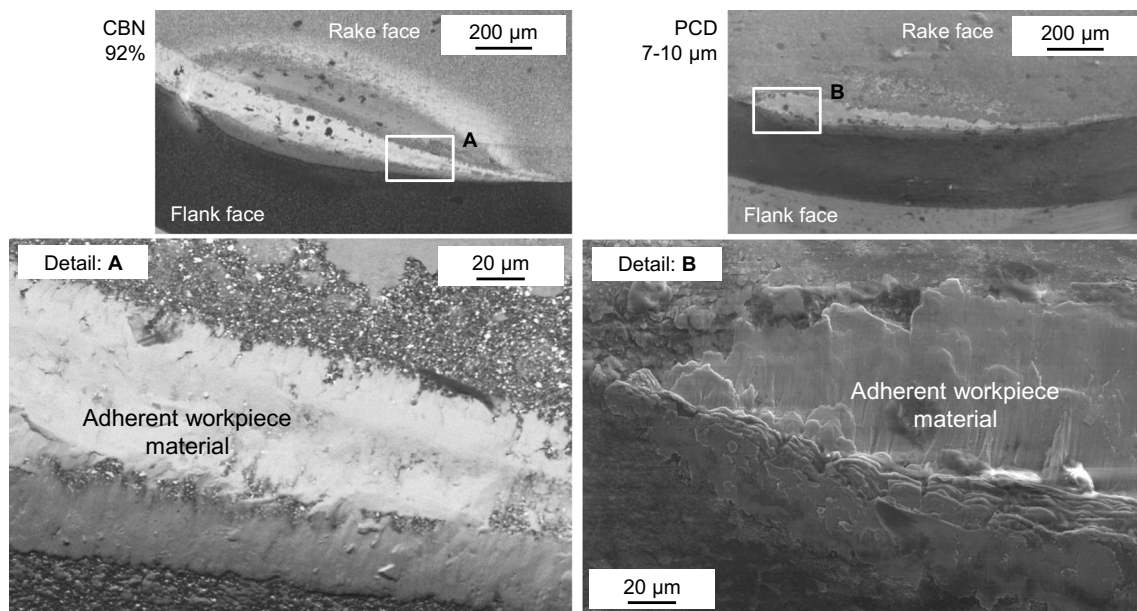


**Fig. 6** Adherent workpiece material on worn CBN and PCD cutting inserts

by using PCD tools with 7–10- and 2- $\mu\text{m}$  grain sizes. As shown in Fig. 5, limited differences in tool wear evolution between 7–10- and 2- $\mu\text{m}$  grain sizes were noticed. The abrasive wear mechanism of PCD cutting tools is dominated by cleavage/breaking of individual grains of diamond on microscopic scale [33]. Moreover, the high-magnification pictures obtained by means of SEM (in Fig. 6) highlight that adhesion of workpiece material on the wear scar was detected [44, 45].

### 3.2 Main properties of PCD cutting material

It is well known from literature that, for PCD tools, each combination of grain size and microstructure results in specific mechanical/thermal properties and wear resistance [33]. In order to better explain the experimental evidences, characterization tests for PCD tool materials were made. The typical elemental composition as well as the microstructures is shown in Fig. 7.

**Fig. 7** Microstructures and elemental composition of PCD material

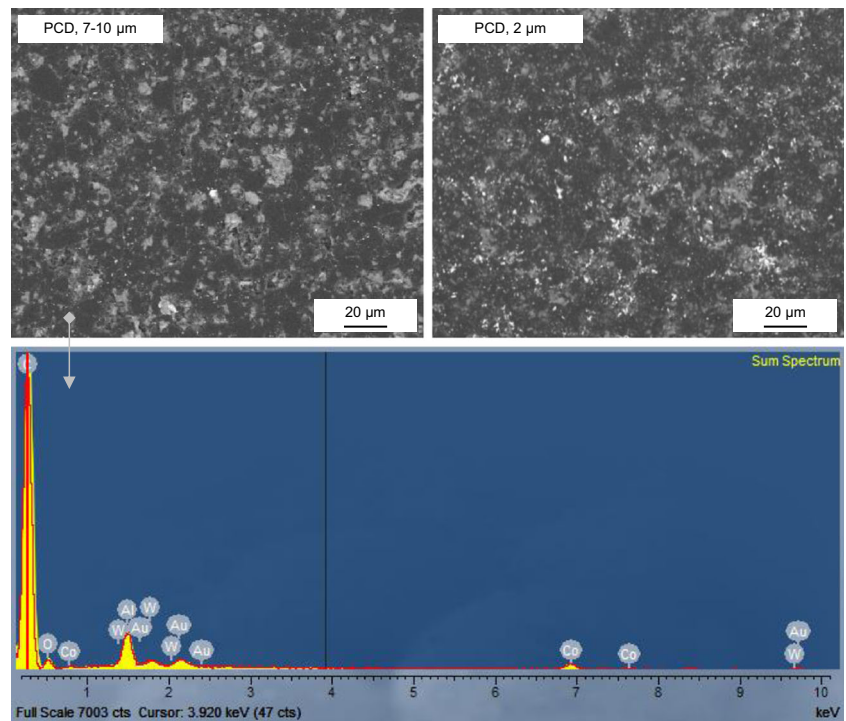




**Table 1** Mechanical properties of PCD cutting materials

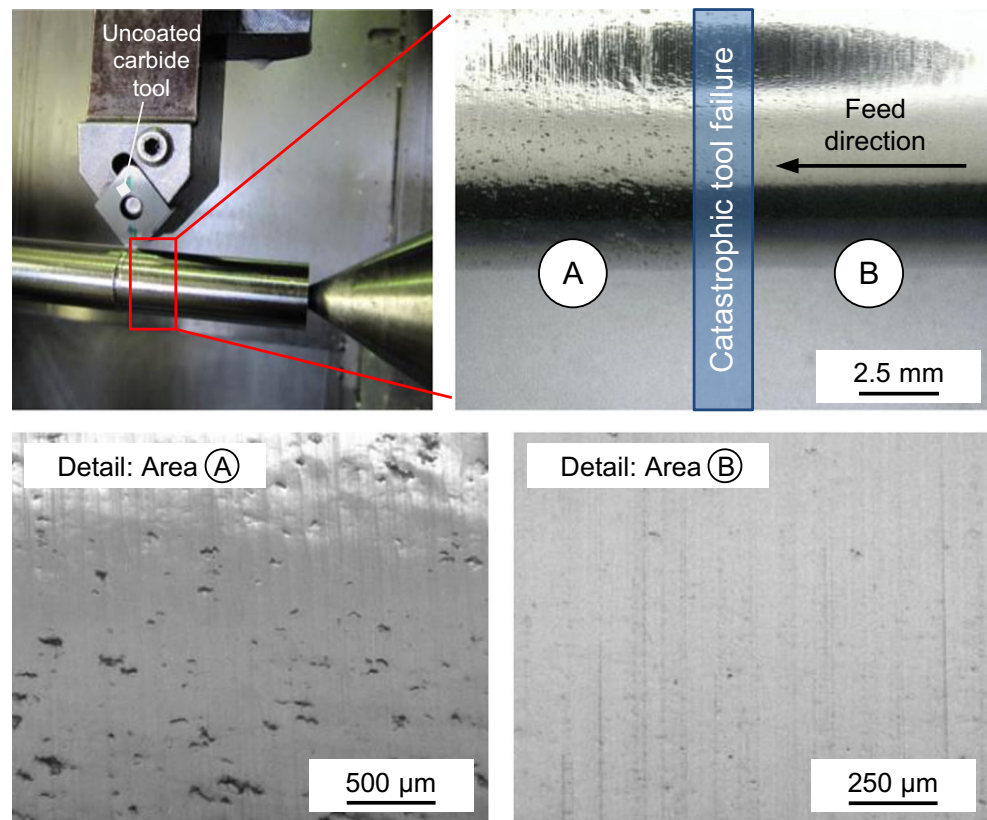
PCD grain size ( $\mu\text{m}$ )	Vickers hardness (HV)		Young modulus (GPa)	
	Average	Std. dev.	Average	Std. dev.
2	6597	1513	612	115
7–10	7442	634	627	68

As far as the elemental composition is concerned, yellow spectrum shows the peaks directly obtained during the acquisition, while the red line corresponds to the theoretical spectrum reconstruction, after the peak assignation, obtained by software. The spectrum evidences the presence of carbon, oxygen, tungsten, and cobalt. The gold arises from the layer (of few nanometer in thickness) sputtered on the surface prior to the sample analysis, aimed to prevent an electrical charging of the insulating material. The amount of aluminum, tungsten, and cobalt ranges between 2 and 3 at.% for all the samples. Therefore, the semiquantitative analysis does not show any significant difference in terms of binder content, so that no influence on the thermal properties is expected to arise from the amount of metals in tool materials. On that basis, thermal conductivity should depend only on diamond particle size, which increase is known to enhance the conductivity. However, no significant differences are expected increasing the size from 2 to 7–10  $\mu\text{m}$  [46]. Vickers hardness and Young

modulus for PCD cutting tools are listed in Table 1. PCD inserts of 2- and 7–10- $\mu\text{m}$  grain sizes show comparable hardness average values, since the difference is not statistically different. Two-micrometer PCD has the highest standard deviation because of the difficulty, arising from the grain size, to limit the measurement only to diamond particles that are embedded in the binder. As far as the Young modulus is concerned, the same consideration can be done: 2- $\mu\text{m}$  PCD and 7–10- $\mu\text{m}$  PCD present comparable average values. Such results are in agreement with the unmeaning differences observed in tool wear curves (Fig. 5).

### 3.3 Surface quality/integrity results

During each cutting test, roughness was monitored by means of a portable tester. Measurements were sampled after each cutting pass, until reaching the end-of-tool life criterion. For all the tests, the average values of the roughness indices were lower than 0.4 and 3  $\mu\text{m}$  for  $R_a$  and  $R_z$ , respectively. For PCD tools,  $R_a$  was 0.28  $\mu\text{m}$  and  $R_z$  was 1.8  $\mu\text{m}$ . For CBN tools,  $R_a$  was 0.24  $\mu\text{m}$  and  $R_z$  was 1.5  $\mu\text{m}$ . The catastrophic tool failure negatively affects the surface integrity of machined components, particularly when using uncoated carbide inserts. As soon as the tool is no longer sharp, a visible worsening of the workpiece machined surface occurs, with the appearance of numerous surface cracks (Fig. 8). Owing to CBN and PCD high hardness and high melting point, high-performance tools

**Fig. 8** Effects of tool failure on surface integrity

withstand the heat and pressure developed during cutting without compromising surface integrity of the machined component, because of their ability to maintain a sharp cutting edge for longer periods [47, 48]. Figure 9 shows SEM pictures of the surfaces machined using PCD tools (i.e., the cutting material suitable for attaining the highest tool life). At the end of tool life, surface quality is acceptable, with a limited amount of defects. These ones, according to the previous investigations, could be hypothetically traced back to the presence of borides [31, 32]. Furthermore, crack density is low. In comparison to literature [17, 18], the size of the defects is quite small, being the length in the order of a few tens of microns.

### 3.4 Cryogenic-assisted turning applying PCD tools

Turning tests under traditional wet conditions and characterization data indicated that the differences between 2- $\mu\text{m}$  PCD and 7–10- $\mu\text{m}$  PCD are poorly relevant. Based on this similarity, only one type of PCD was considered for cryogenic-assisted tests. Figure 10 presents the results of turning trials carried out with 7–10- $\mu\text{m}$  PCD tools and applying cryogenic cooling with liquid nitrogen (boiling point,  $-196^\circ\text{C}$ ). In comparison to conventional flood cooling, with cryogenic-assisted cutting, a significant increase in tool life was achieved, up to  $T_L \approx 30$  min (assuming the tool wear limit criterion of  $V_{B\max} = 100\ \mu\text{m}$ ). As shown by  $R_a$  values, roughness rises with the increase of tool wear.

The high thermal conductivity of PCD prevents a high heat accumulation on the cutting edge, and the extremely low temperature of the cooling medium ( $\text{LN}_2$ ) increases the thermal gradient between cutting zone and tool, with a higher heat removal and a huge reduction of thermal load [49, 50]. In addition, the use of an adapted nozzle directing the coolant supply at the tool/workpiece/chip interface should intensify the cooling effect, being the thermo-dynamical impact of the expanding liquid nitrogen close to the cutting zone [51]. An improvement in performance of machined components

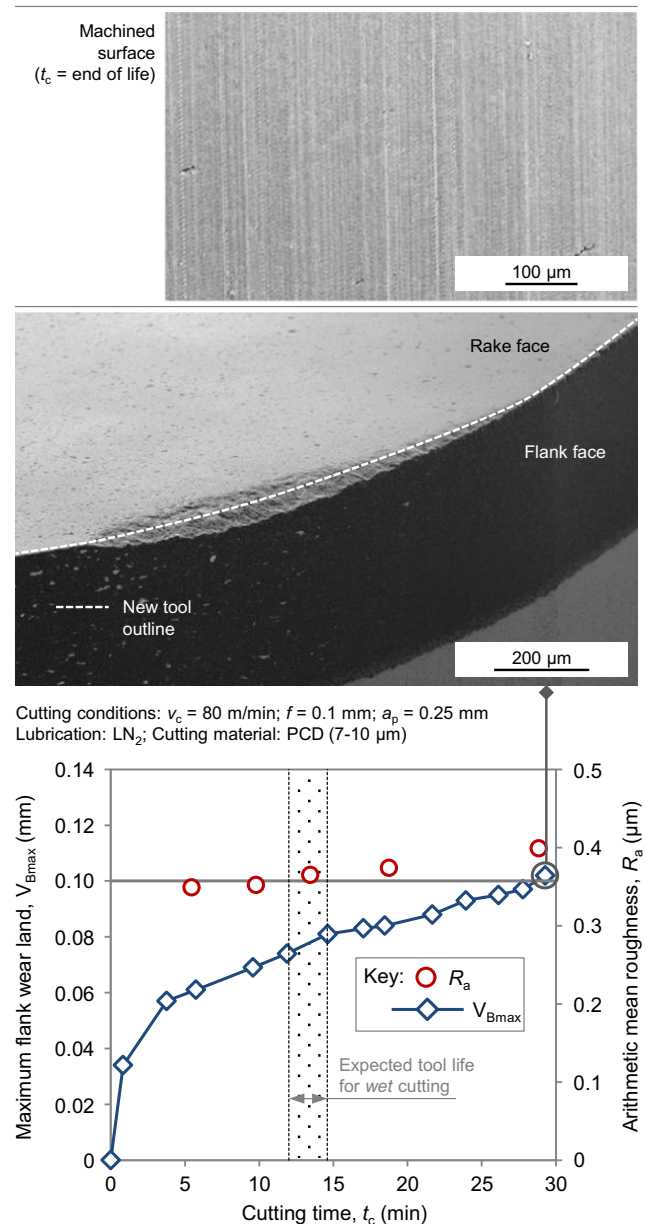


**Fig. 10** Typical results for cryogenic-assisted turning of TNM alloy with PCD tools

Cutting conditions:  $v_c = 80\ \text{m/min}$ ;  $f = 0.1\ \text{mm}$ ;  $a_p = 0.25\ \text{mm}$ ; WET cutting (emulsion). Tool: PCD (7–10  $\mu\text{m}$ )

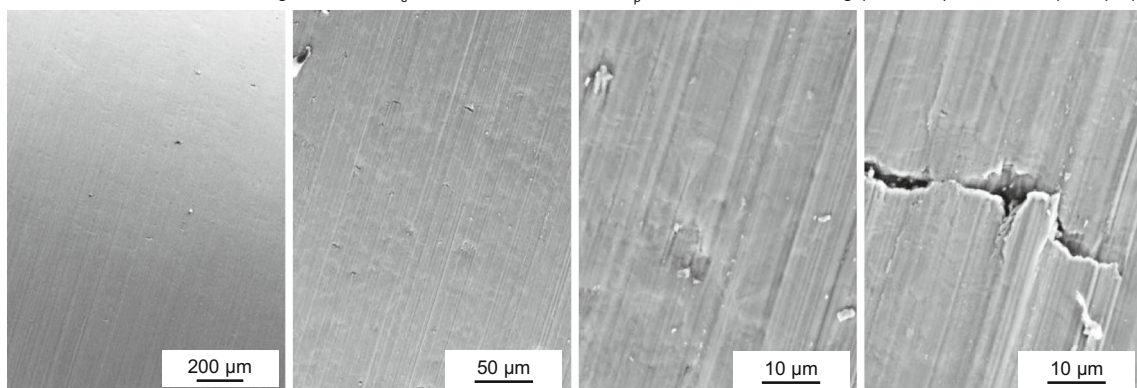


**Fig. 9** SEM observations of machined surfaces, at the end of tool life ( $V_{B\max} = 100\ \mu\text{m}$ ), when applying PCD cutting inserts



through a superior surface integrity characteristic is expected [52]. As already discussed in [32], a hardened layer below the surface appears when turning titanium aluminides. The increase in subsurface hardness indicates the susceptibility of the workpiece material to strain hardening. When the tool wear increases, the thermal and mechanical load increases too. With cryogenic cooling, due to the reduction of the tool wear, a reduction of the measured subsurface hardness values (which corresponds to the reduction of the depth of subsurface microstructural alterations) was detected [32].

#### 4 Conclusions and outlooks

Longitudinal external turning tests were performed on an investment-casted and HIPed TNM gamma titanium aluminide, adopting finishing process parameters. The performance of CNMA 120424 uncoated and (AlCrN- and TiAlN-) coated ISO K10 grade carbide tools was compared to that of CBN and PCD cutting inserts, under standard flood cooling lubrication (a 6 % emulsion of cutting oil in water). The CBN content was varied from 50 to 92 %, with TiN or TiC binders, while PCD was characterized by a fine grain size of 2 or 7–10  $\mu\text{m}$ .

Experimental results proved that tool failure was suddenly reached when using coated carbide and low-content CBN inserts. At fixed cutting conditions, the tool life of approximately 2 min achieved with uncoated carbide tools can be extended to 7.2 min with 92 % content CBN tools and to about 14 min by using PCD tools with 7–10- and 2- $\mu\text{m}$  grain size (assuming  $V_{B\text{max}}=0.1$  mm as tool wear limit). Overall, high-performance cutting tools can improve machining productivity due to the outstanding thermal conductivity, high hardness, and wear resistance. The poorly significant differences in tool wear results between 2- $\mu\text{m}$  PCD and 7–10- $\mu\text{m}$  PCD inserts should be traced back to the limited differences in cutting material properties, as supported by the characterization data.

Tool wear directly affects surface quality results. When the tool wears, the worsening of machined surfaces occurs and surface defects as microcracks appear (in some cases likely due to the presence of titanium diborides within the workpiece microstructure). CBN and PCD are suitable to withstand the heat and pressure developed during material removal without compromising surface integrity, because of their ability to retain a sharp cutting edge for longer cutting time. Moreover, tool life can be enhanced applying cooling strategies to effectively remove heat from the cutting area. When using 7–10- $\mu\text{m}$  PCD inserts, characterized by high thermal conductivity, and increasing the thermal gradient by exploiting the expansion of liquid nitrogen directly supplied on the tool rake face, the heat accumulation on the cutting edge is reduced, further increasing the tool life.

**Acknowledgments** The authors thank the European Union for funding the research activities under the Ziel 2 Programm 2007–2013 (EFRE), Grant Number 30 00 240 02 (ManufacTiAl project), and the Federal State of NRW for the financial support. Access e.V. Techcenter (Aachen, Germany) and Dr.-Ing. Martin Arft are also kindly acknowledged for the technical support during the project development.

#### References

1. Clemens H, Mayer S (2014) Development status, applications and perspectives of advanced intermetallic titanium aluminides. *Mater Sci Forum* 783–786:15–20
2. Cheng TT, Willis MR, Jones IP (1999) Effects of major alloying additions on the microstructure and mechanical properties of  $\gamma$ -TiAl. *Intermetallics* 7:89–99
3. Kothari K, Radhakrishnan R, Wereley NM (2012) Advances in gamma titanium aluminides and their manufacturing techniques. *Prog Aerosp Sci* 55:1–16
4. Djanarthany S, Viala J-C, Bouix J (2001) An overview of monolithic titanium aluminides based on  $\text{Ti}_3\text{Al}$  and TiAl. *Mater Chem Phys* 72:301–319
5. Austin CM (1999) Current status of gamma Ti aluminides for aerospace applications. *Curr Opin Solid State Mater Sci* 4:239–242
6. Tetsui T (1999) Gamma Ti aluminides for non-aerospace applications. *Curr Opin Solid State Mater Sci* 4:243–248
7. Weinert K, Bergmann S, Kempmann C (2006) Machining sequence to manufacture a  $\gamma$ -TiAl-conrod for application in combustion engines. *Adv Eng Mater* 8:41–47
8. Gebauer K (2006) Performance, tolerance and cost of TiAl passenger car valves. *Intermetallics* 14:355–360
9. Larsen DE Jr (1996) Status of investment cast gamma titanium aluminides in the USA. *Mater Sci Eng A* 213:128–133
10. Wang YH, Lin JP, He YH, Wang YL, Chen GL (2009) Microstructural characteristics of Ti-45Al-8.5Nb/TiB<sub>2</sub> composites by powder metallurgy. *J Alloys Compd* 468:505–511
11. Appel F, Oehring M, Paul JDH, Klinkenberg C, Carneiro T (2004) Physical aspects of hot-working gamma-based titanium aluminides. *Intermetallics* 12:791–802
12. Tetsui T, Shindo K, Kaji S, Kobayashi S, Takeyama M (2005) Fabrication of TiAl components by means of hot forging and machining. *Intermetallics* 13:971–978
13. Aspinwall DK, Dewes RC, Mantle AR (2005) The machining of  $\gamma$ -TiAl intermetallic alloys. *CIRP Ann Manuf Technol* 54:99–104
14. Pramanik A (2014) Problems and solutions in machining of titanium alloys. *Int J Adv Manuf Technol* 70:919–928
15. Hood R, Aspinwall DK, Soo SL, Mantle AL, Novovic D (2014) Workpiece surface integrity when slot milling  $\gamma$ -TiAl intermetallic alloy. *CIRP Ann Manuf Technol* 63:53–56
16. Kolahdouz S, Hadi M, Arezoo B, Zamani S (2015) Investigation of surface integrity in high speed milling of gamma titanium aluminide under dry and minimum quantity lubricant conditions. *Procedia CIRP* 26:367–372
17. Sharman ARC, Aspinwall DK, Dewes RC, Bowen P (2001) Workpiece surface integrity considerations when finish turning gamma titanium aluminide. *Wear* 249:473–481
18. Mantle AL, Aspinwall DK (2001) Surface integrity of a high speed milled gamma titanium aluminide. *J Mater Process Technol* 118: 143–150
19. Sharman ARC, Aspinwall DK, Dewes RC, Clifton D, Bowen P (2001) The effects of machined workpiece surface integrity on the fatigue life of  $\gamma$ -titanium aluminide. *Int J Mach Tools Manuf* 41: 1681–1685

20. Mantle AL, Aspinwall DK (1997) Surface integrity and fatigue life of turned gamma titanium aluminide. *J Mater Process Technol* 72: 413–420
21. Uhlmann E, Schauerte OS, Brücher M, Herter S (2001) Tool wear during turning of titanium aluminide intermetallics. *Prod Eng VIII/2*:13–16
22. Beranoagire A, López de Lacalle LN (2011) Turning of gamma TiAl intermetallic alloys. *Proc 4th Manuf Eng Soc Int Conf AIP Conf Proc* 1431:526–532
23. Vargas Pérez RG (2005) Wear mechanisms of WC inserts in face milling of gamma titanium aluminides. *Wear* 259:1160–1167
24. Mantle AL, Aspinwall DK (2006) Cutting force evaluation when high speed end milling a gamma titanium aluminide intermetallic alloy. In: Morris DG, Naka S, Caron P (eds) *Intermetallics and superalloys 10*. Wiley-VCH Verlag GmbH & Co
25. Beranoagire A, López de Lacalle LN (2010) Optimising the milling of titanium aluminides alloys. *Int J Mechatron Manuf Syst* 3: 425–436
26. Beranoagire A, Olvera D, López de Lacalle LN (2012) Milling of gamma titanium-aluminum alloys. *Int J Adv Manuf Technol* 62: 83–88
27. Aspinwall DK, Mantle AL, Chan WK, Hood R, Soo SL (2013) Cutting temperatures when ball nose end milling  $\gamma$ -TiAl intermetallic alloys. *CIRP Ann Manuf Technol* 62:75–78
28. Beranoagire A, Olvera D, Urbicain G, López de Lacalle LN, Lamikiz A (2010) Hole making in gamma TiAl. *DAAAM Int Sci Book* 2010:337–346
29. Zhu L, Chen X, Viehweger B (2010) Preliminary study on deep-hole drilling gamma titanium aluminide. *Adv Mater Res* 139–141: 831–834
30. Zhu L, Chen X, Viehweger B (2011) Experimental study on deep hole drilling gamma titanium aluminide. *Key Eng Mater* 455:293–296
31. Settineri L, Priarone PC, Arft M, Lung D, Stoyanov T (2014) An evaluative approach to correlate machinability, microstructures, and material properties of gamma titanium aluminides. *CIRP Ann Manuf Technol* 63:57–60
32. Klocke F, Settineri L, Lung D, Priarone PC, Arft M (2013) High performance cutting of gamma titanium aluminides: influence of lubricoolant strategy on tool wear and surface integrity. *Wear* 302: 1136–1144
33. Sadik IM (2013) An introduction to cutting tools materials and applications. Sandvik Coromant. Printed by Elanders, Sweden. ISBN 978-91-637-4920-9
34. Nurul Amin AKM, Ismail AF, Nor Khairusshima MK (2007) Effectiveness of uncoated WC-Co and PCD inserts in end milling of titanium alloy-Ti-6Al-4V. *J Mater Process Technol* 192–193: 147–158
35. Ferraris E, Mestrom T, Bian R, Reynaerts D, Lauwers B (2012) Machinability investigation on high speed hard turning of ZrO<sub>2</sub> with PCD tools. *Procedia CIRP* 1:500–505
36. Dolda C, Henerichs M, Bochmann L, Wegener K (2012) Comparison of ground and laser machined polycrystalline diamond (PCD) tools in cutting carbon fiber reinforced plastics (CFRP) for aircraft structures. *Procedia CIRP* 1:178–183
37. Philbin P, Gordon S (2005) Characterisation of the wear behaviour of polycrystalline diamond (PCD) tools when machining wood-based composites. *J Mater Process Technol* 162–163:665–672
38. Cook MW, Bossom PK (2000) Trends and recent developments in the material manufacture and cutting tool application of polycrystalline diamond and polycrystalline cubic boron nitride. *Int J Refract Met Hard Mater* 18:147–152
39. Costes JP, Guillet Y, Poulachon G, Dessoly M (2007) Tool-life and wear mechanisms of CBN tools in machining of Inconel 718. *Int J Mach Tools Manuf* 47:1081–1087
40. Poulachon G, Bandyopadhyay BP, Jawahir IS, Pheulpin S, Seguin E (2004) Wear behavior of CBN tools while turning various hardened steels. *Wear* 256:302–310
41. Aguilar J, Schievenbusch A, Kätzlitz O (2011) Investment casting technology for production of TiAl low pressure turbine blades—process engineering and parameter analysis. *Intermetallics* 19:757–761
42. Klocke F, Lung D, Arft M, Priarone PC, Settineri L (2013) On high-speed turning of a third-generation gamma titanium aluminide. *Int J Adv Manuf Technol* 65:155–163
43. Klocke F (2011) *Manufacturing processes 1—cutting*. RWTH Edition, Springer-Verlag Berlin Heidelberg
44. Priarone PC, Robiglio M, Settineri L, Tebaldo V (2015) Effectiveness of minimizing cutting fluid use when turning difficult-to-cut alloys. *Procedia CIRP* 29:341–346
45. Priarone PC, Rizzuti S, Settineri L, Vergnano G (2012) Effects of cutting angle, edge preparation, and nano-structured coating on milling performance of a gamma titanium aluminide. *J Mater Process Technol* 212:2619–2628
46. Ekimov EA, Suetin NV, Popovich AF, Ralchenko VG (2008) Thermal conductivity of diamond composites sintered under high pressures. *Diam Relat Mater* 17:838–843
47. Ezugwu EO, Da Silva RB, Bonney J, Machado AR (2005) Evaluation of the performance of CBN tools when turning Ti-6Al-4V alloy with high pressure coolant supplies. *Int J Mach Tools Manuf* 45:1009–1014
48. Zoya ZA, Krishnamurthy R (2000) The performance of CBN tools in the machining of titanium alloys. *J Mater Process Technol* 100: 80–86
49. Yildiz Y, Nalbant M (2008) A review of cryogenic cooling in machining processes. *Int J Mach Tools Manuf* 48:947–964
50. Wang ZY, Rajurkar KP (2000) Cryogenic machining of hard-to-cut materials. *Wear* 239:168–175
51. Bermingham MJ, Palanisamy S, Kent D, Dargusch MS (2012) A comparison of cryogenic and high pressure emulsion cooling technologies on tool life and chip morphology in Ti-6Al-4V cutting. *J Mater Process Technol* 212:752–765
52. Kaynak Y, Lu T, Jawahir IS (2014) Cryogenic machining-induced surface integrity: a review and comparison with dry, MQL, and flood-cooled machining. *Mach Sci Technol* 18:149–198